Development 140, 1517-1527 (2013) doi:10.1242/dev.087593

Intradermal adipocytes mediate fibroblast recruitment during skin wound healing

Barbara A. Schmidt and Valerie Horsley*

SUMMARY

Acute wound healing in the skin involves the communication of multiple cell types to coordinate keratinocyte and fibroblast proliferation and migration for epidermal and dermal repair. Many studies have focused on the interplay between hematopoietic cells, keratinocytes and fibroblasts during skin wound healing, yet the possible roles for other cell types within the skin, such as intradermal adipocytes, have not been investigated during this process. Here, we identify that adipocyte lineage cells are activated and function during acute skin wound healing. We find that adipocyte precursor cells proliferate and mature adipocytes repopulate skin wounds following inflammation and in parallel with fibroblast migration. Functional analysis of mice with defects in adipogenesis demonstrates that adipocytes are necessary for fibroblast recruitment and dermal reconstruction. These data implicate adipocytes as a key component of the intercellular communication that mediates fibroblast function during skin wound healing.

KEY WORDS: Adipocytes, Fibroblasts, Skin, Wound healing, Regeneration, Mouse

INTRODUCTION

Acute wound healing in the skin requires communication between multiple cell types to restore its barrier function by coordinating keratinocyte re-epithelialization and the restructuring of the dermis by fibroblasts (Leibovich and Ross, 1975; Wu et al., 1997). In the initial stages of wound healing, immune cells clear foreign pathogens (Ross and Odland, 1968; Simpson and Ross, 1972) and produce growth factors (Leibovich and Ross, 1975; Wu et al., 1997) that activate keratinocytes, endothelial cells and fibroblasts. These cells proliferate and migrate to reseal the epidermal barrier and reform the dermal structure (Sunderkötter et al., 1994; DiPietro, 1995). The final processes of extracellular matrix remodeling continue for several weeks following wounding.

We recently found that resident intradermal adipocytes regenerate in the skin during hair cycling and that adipocyte lineage cells are required for progression of native hair follicle regeneration (Festa et al., 2011). Although adipocytes are primarily known for their role in the storage of triglycerides as an energy source, they also function as endocrine cells that secrete growth factors and cytokines associated with several physiological processes, including glucose and lipid metabolism (Kilroy et al., 2007; Ouchi et al., 2011). However, whether intradermal adipocytes regenerate or function during skin wound healing is not known.

Here, we identify the activation and function of adipocyte lineage cells during acute skin wound healing. We demonstrate that adipocyte precursors proliferate and mature intradermal adipocytes repopulate the skin after wounding. Surprisingly, we find that genetic and pharmacological inhibition of mature adipocyte formation abrogates fibroblast presence and extracellular matrix protein deposition in the regenerating dermis. These defects result in long-term loss of skin integrity and in wound recurrence. Together, these results demonstrate that the proliferative stage of skin wound healing requires adipocytes to direct fibroblast function.

Yale University, Department of Molecular, Cellular and Developmental Biology, New Haven, CT 06520, USA.

*Author for correspondence (valerie.horsley@yale.edu)

Accepted 17 January 2013

MATERIALS AND METHODS

Animal experiments

All animals were handled according to the institutional guidelines of Yale University. CD-1, FVB, AZIP and ob/ob mice were described previously (Moitra et al., 1998; Chua et al., 1996; Campfield et al., 1995). For experiments using AZIP and ob/ob mice, we used age- and sex-matched littermates or FVBs as controls.

For wounding studies, a full-thickness 4 mm wound was introduced by punch biopsy onto the middle backskin of 7-week-old adult male mice. For each time point examined, three to six mice were used with a minimum of four wounds per mouse. Each wound was spaced at least 2 mm apart on the backskin. The wounded skin area and no more than 1 mm of surrounding unwounded skin was excised for mRNA and protein analysis.

For 5-bromo-2′-deoxyuridine (BrdU) pulse experiments, mice were injected intraperitoneally with 50 mg/kg BrdU (Sigma-Aldrich) daily for 2 days prior to being sacrificed. For experiments using GW9662 (Cayman Chemical), mice were injected daily at 1 μg/g at the indicated time points. For experiments using bisphenol A diglycidyl ether (BADGE) (Cayman Chemical), mice were injected daily at 15 μg/g. Vehicle controls were injected with the same amount of DMSO.

Histology and immunofluorescence

For histological analysis, 14 μm sections from the central part of the wound were fixed in 4% formaldehyde and stained with Hematoxylin and Eosin. To measure histological characteristics of wounds, each wound was embedded and sectioned through its entirety. Sections from the middle of the wound, as indicated by the greatest length of hyperproliferative epidermis, were used for all analyses. We determined the percentage of epidermal re-epithelialization by measuring the total length of the hyperproliferative keratinocyte region and dividing by the total wound length (the sum of the lengths of the epithelium and unepithelialized wound bed). The length and area of the hyperproliferative wound epithelium were determined using ImageJ software (NIH). To analyze collagen protein, trichrome staining was performed using Masson's Trichrome Stain Kit according to the manufacturer's protocol (Polysciences).

For immunofluorescence, the following antibodies were used: perilipin A (rabbit, Abcam, 1:1000); ER-TR7 (rat, Novus Biologicals, 1:300); α-SMA (mouse, Thermo Scientific, 1:300); BrdU (rat, Abbiotec, 1:300); LY6G (rat, Novus Biologicals, 1:50); F4/80 (rat, Abcam, 1:100); CD45 (rat, eBiosciences, 1:300); GS-IB4 Alexa 488-conjugated (Invitrogen, 1:200); vimentin (rabbit, Cell Signaling, 1:100); and KI67 (rabbit, Leica, 1:300). When applicable, the M.O.M. Kit (Vector Labs) was used to prevent nonspecific binding with mouse antibodies. Fluorescence quantification was

performed using ImageJ. Corrected total fluorescence (CTF) was calculated by determining the integrated density of fluorescence in the wound bed or adjacent non-wounded area (NW) in the same slide and subtracting the total area of the region multiplied by the mean background fluorescence of the negative epidermis in the slide of interest (Gavet and Pines, 2010).

Flow cytometry analysis

Dermal cells were released from skin tissue by digestion of minced tissue with 1:100 collagenase IA (Sigma). Adipocyte precursor cell purification was performed as described (Festa et al., 2011). Briefly, single-cell suspensions were resuspended in FACS staining buffer comprising 4% fetal bovine serum (FBS) in PBS and stained with antibodies. Cells were fixed and permeabilized using BD fixation/permeabilization buffers (BD Biosciences). Myofibroblast and immune cell analysis was performed using α-SMA-FITC (Abcam) and CD45-PE-Cy7 (eBiosciences). FITC-conjugated isotype controls were used for intracellular staining at the same concentration (FITC mouse IgG2a, BD Pharmingen). Macrophages were isolated using CD-45-PE-Cy7 (eBiosciences), CD11b-PE (BD Biosciences) and F4/80-APC (Biolegend). Cells were sorted using a FACS Aria III equipped with FACS DiVA software (BD Biosciences). BrdU staining of cells was performed according to manufacturer's directions using the BrdU Flow Kit (BD Biosciences).

In vitro assays and cell culture

Cell culture migration experiments were performed using primary fibroblasts from mouse tail skin. Sections (1 cm^2) of mouse tail skin were placed in culture dishes and grown in fibroblast medium [(DMEM high-glucose medium containing 10% FBS, 1× penicillin/streptomycin/amphotericin B Solution (PSA)]. GW9662 or DMSO was added at 2 μM, 5 μM or 10 μM. Migration distance was measured from the edge of the tail skin after 3 and 6 days using ImageJ. For conditioned medium (CM) experiments, 50,000 total dermal cells or FACS-purified adipocyte precursors were plated in fibroblast medium as described (Festa et al., 2011). After 3 days, adipocytes were evident in adipocyte cultures and CM was collected daily. Skin explants were plated for 1 day prior to the addition of CM. Migration distance was measured from the edge of the tail skin after 3, 4 and 5 days using ImageJ. To analyze proliferation, fibroblasts were pulsed for 3 hours with BrdU at the indicated days, fixed and permeabilized using the BD fixation/permeablization buffers and analyzed on a FACS Aria.

RT-PCR

For expression analysis from skin, 4 mm skin wounds were excised from skin using 5 mm biopsy punches. The wounds and surrounding tissue were homogenized in TRIzol (Invitrogen) and RNA was extracted according to the manufacturer's instructions. Primers (5′-3′, forward and reverse): fibronectin, CTACCCTGCAGCCTCTGCGC and TCACCTCCCT-GGCTCGGTCG; collagen Iα1, TGTTCGTGGTTCTCAGGGTAG and TTGTCGTAGCAGGGTTCTTTC; collagen IIIα1, TGCCCACAGC-CTTCTACACCT and CCAGCTGGGCCTTTGATACCT; *Tgfb*, GGATACCAACTATTGCTTCAGCTCC and AGGCTCCAAATATA-GGGGCAGGGTC; *Pdgfa*, GCGGTGGTGGACCCGTGAAG and CCGGGAGTTGATCGAGCGGC; *Mmp9*, ATCCCCAGAGCGTCAT-TCGCG and CACGTAGCCCACGTCGTCCAC; *Il10*, GCCCAGAAAT-CAAGGAGCATT and TGCTCCACTGCCTTGCTCTTA. RT-PCR was performed on a LightCycler 480 (Roche) as described previously (Festa et al., 2011). All results were normalized to β-actin values.

RNA from macrophages was isolated using TRIzol (Invitrogen) according to manufacturer's instructions.

Western blot

Skin wounds from GW9662-injected and vehicle-injected mice were excised using 5 mm biopsy punches and protein was isolated using RIPA lysis buffer. Protein concentration was analyzed using the BCA Protein Assay Kit (Thermo Scientific). Primary antibodies used were fibronectin (Calbiochem, 1:400), α-SMA (Sigma, 1:2000) and β-actin (Sigma, 1:10,000). Secondary antibodies used were peroxidase-conjugated goat anti-mouse IgG (Jackson Immunoresearch; 1:5000) and peroxidase-conjugated goat anti-rabbit IgG (Jackson Immunoresearch; 1:5000). Western blots were developed using ECL Plus Detection System (GE Healthcare).

Statistics

To determine significance between groups, comparisons were made using Student's *t*-test and one-way ANOVA with GraphPad Prism. $P<0.05$ was accepted for statistical significance.

RESULTS

Adipocytes repopulate skin wounds during the proliferative phase of healing

To determine whether adipocytes repopulate skin wounds, we analyzed mature adipocytes during a timecourse of full-thickness wound healing following punch biopsy of murine dorsal skin. Skin sections of a wound healing timecourse were immunostained with antibodies against the adipocyte marker perilipin A (perilipin 1 – Mouse Genome Informatics) (Festa et al., 2011; Greenberg et al., 1991). We find that small perilipin$^+$ adipocytes are present in the wound after re-epithelialization at 5 days (Fig. 1A,B).

To confirm that adipocytes exist in skin wounds, we analyzed wounds from mice expressing Cre recombinase under the control of the adiponectin promoter (*adiponectinCre*) crossed to the fluorescent membrane tdTomato/membrane eGFP (*mT/mG*) reporter strain, which marks Cre excision by a heritable switch from tdTomato expression to eGFP expression in an adipocyte-specific manner (Muzumdar et al., 2007; Eguchi et al., 2011). Numerous small, GFP-expressing cells are apparent within the wound bed at both 5 and 7 days after wounding (Fig. 1C). These data were confirmed by analysis of isolated cells by flow cytometry. Analysis of GFP expression in isolated dermal cells revealed that 24% of the isolated cells were GFP$^+$ in non-wounded skin and increased to 47% 5 days after wounding (Fig. 1C). Taken together, these data indicate that small, mature adipocytes reappear in the wound bed following skin injury.

To define the timing of adipocyte presence in skin wounds, we analyzed perilipin$^+$ adipocytes with reference to immune cells, endothelial cells and fibroblasts by immunostaining skin sections 5 and 7 days following wounding with antibodies against perilipin, CD45 (PTPRC – Mouse Genome Informatics), GS-IB4 and ER-TR7 (Brack et al., 2007) to mark immune, endothelial and fibroblast cells, respectively. Perilipin$^+$ adipocytes were localized at the wound edge after 5 days, in contrast to the CD45$^+$ immune cells which filled the middle of the wound bed. Small, mature adipocytes appeared adjacent to ER-TR7$^+$ fibroblasts and GS-IB4$^+$ blood vessels at the wound edge at day 5 and within the center of the wound bed by day 7 (Fig. 1D). Thus, adipocytes repopulate skin wounds after inflammation and during fibroblast and endothelial cell recruitment.

We have shown that adipocyte precursor cells, which lack hematopoietic and endothelial markers (Lin$^-$) but express CD34, CD29 (ITGβ1 – Mouse Genome Informatics) and SCA1 (LY6A – Mouse Genome Informatics), have adipogenic potential and are resident in adipose depots and the skin (Rodeheffer et al., 2008; Festa et al., 2011). Furthermore, these adipocyte precursors are activated to proliferate during hair cycle-associated adipocyte regeneration in the skin (Festa et al., 2011). To determine whether the activation of adipocyte precursors occurs following wounding, we analyzed the presence and proliferation of Lin$^-$, CD34$^+$, CD29$^+$, SCA1$^+$ cells 5 days after skin injury by FACS. We pulsed mice with BrdU for 48 hours prior to each time point and isolated adipocyte precursors from wounded skin. We found that the percentage and proliferation of adipocyte precursors increased in wounds after 5 and 7 days compared with unwounded skin (Fig. 2A-C). These data demonstrate that resident adipocyte precursor cells are activated to proliferate during wounding.

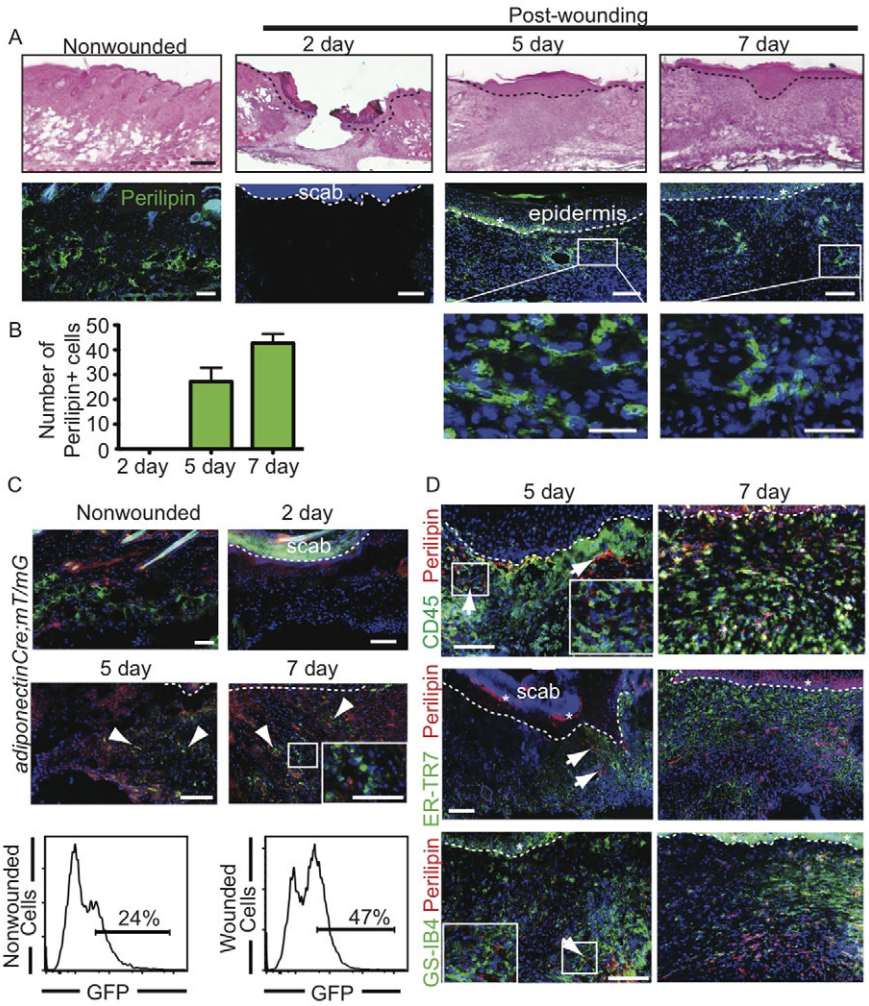

Fig. 1. Adipocytes repopulate skin wounds. (**A**) Histological analysis of adipocyte formation during wound healing. Skin sections stained with Hematoxylin and Eosin (H&E) reveal wound histology (top row). Immunostaining with antibodies against perilipin A (green) reveals the presence of adipocytes within wounds at 5 and 7 days (middle and bottom rows). Dotted line indicates the epidermis/dermis boundary. Asterisk indicates background fluorescent staining. The boxed areas are magnified beneath. (**B**) Quantitation of perilipin$^+$ cells in wound beds at 2, 5 and 7 days after wounding. Mature adipocyte number increases as wounds heal. *n*=4 wounds for each bar per mouse from three mice. Error bars indicate s.e.m. (**C**) Wounds from *adiponectinCre; mT/mG* mice at 2, 5 and 7 days after wounding show GFP$^+$ cells (arrowheads) in the wound bed at 5 and 7 days. Inset shows magnification of boxed area within the same panel. The flow cytometry plots show GFP fluorescence in dermal cells isolated from *adiponectinCre; mT/mG* mice 5 days after wounding or in non-wounded skin. (**D**) Five days after wounding, perilipin$^+$ cells (red) are adjacent to CD45$^+$ immune cells (green), ER-TR7$^+$ activated fibroblasts (green) and GS-IB4$^+$ blood vessels (green). After 7 days, fibroblasts have populated the wound bed with perilipin$^+$ adipocytes. Arrows indicate perilipin$^+$ adipocytes at day 5. Asterisk indicates background staining. Scale bars: 200 μm in A (top); 100 μm in A (middle), C and D; 25 μm in A (bottom) and C (inset).

AZIP mice display defects in fibroblast recruitment into skin wounds

To define the function of adipocytes in wound healing, we analyzed wound healing in the lipoatrophic 'fatless' AZIP/F1 mouse. AZIP mice lack mature white adipocytes throughout the animal, including the skin (Festa et al., 2011), due to the expression of a flag epitope-tagged, dominant-negative form of C/EBP under the control of the aP2 promoter, which normally drives expression of fatty acid binding protein 4 (FABP4) late in adipogenesis. Previously, we found that immature adipocyte lineage cells are present in the skin of AZIP mice (Festa et al., 2011); thus, AZIP mice allow the dissection of the role of mature adipocytes in the skin.

Despite the development of diabetes after 5 weeks of age (Moitra et al., 1998), AZIP mice did not display re-epithelization defects typical of other diabetic models such as ob/ob in the first week of wound healing (Werner et al., 1994; Frank et al., 2000) (Fig. 3A). There was no noticeable defect in wound contraction as determined by the distance between the edges of the panniculus carnosus of AZIP wounds after 1 week compared with controls (Fig. 3B). The normal re-epithelialization of keratinocytes during wound healing in AZIP mice was consistent with similar numbers of BrdU$^+$ keratinocytes in wounds of control and AZIP mice at 3 or 5 days after wounding (Fig. 3C). In addition, immunostaining for F4/80$^+$ (EMR1 – Mouse Genome Informatics) macrophages showed no difference between AZIP mice and littermate controls (Fig. 3D). Thus, keratinocyte and macrophage localization during skin wound healing is unaffected by the lack of mature adipocytes in AZIP mice.

We analyzed Hematoxylin and Eosin (H&E)-stained skin sections of wounds from wild-type (WT) and AZIP mice to determine whether dermal defects occur in AZIP mice. We find that the dermis of AZIP mice at 7 days lacks cellular organization (Fig. 3E). To determine whether fibroblasts were altered in the skin of AZIP mice following wounding, we immunostained skin sections with antibodies against ER-TR7 and α-smooth muscle actin (α-SMA). In WT mice, the wound bed is filled with ER-TR7$^+$ fibroblasts and contains numerous α-SMA$^+$ myofibroblasts after 7 days. By contrast, wound beds of AZIP mice lack cells expressing these markers, suggesting that fibroblast function is altered in healing AZIP skin. This defect does not seem to be a general defect in fibroblast function in AZIP skin, as ER-TR7$^+$ fibroblasts accumulate normally at the wound edge in AZIP mice and non-wounded AZIP skin displays a typical collagen matrix morphology (Fig. 3E, inset).

To determine whether the dermal defects in AZIP mice following wounding are due to a diabetic phenotype, we analyzed wound healing in ob/ob mice, which lack leptin, have increased adipocytes in multiple white adipose depots, and develop diabetes (Ingalls et al., 1950; Mayer and Barrnett, 1953; Zhang et al., 1994). Despite the delay in re-epithelialization in ob/ob mice, fibroblasts and myofibroblasts were present in the wound bed 5 days following wounding (Fig. 3E). To quantitate fibroblast presence in the wound

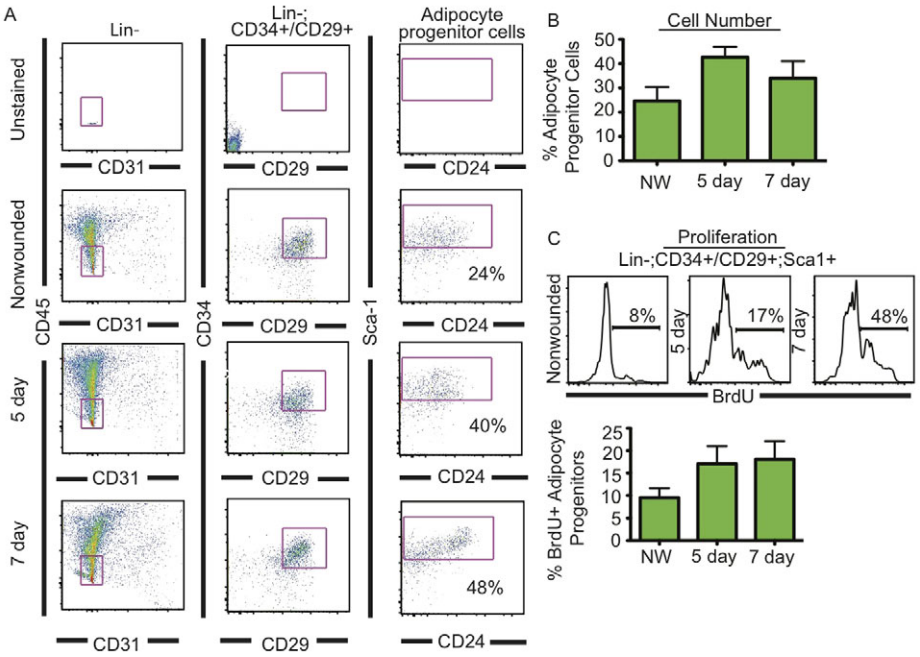

Fig. 2. Adipocyte progenitors proliferate during skin wound healing. (**A**) FACS analysis of adipocyte progenitors in non-wounded and wounded skin tissue at 5 and 7 days after wounding. Biexponential *x* and *y* axes are shown for the Lin$^-$ populations. Percentages of Lin$^-$, CD24$^+$, CD34$^+$ and CD29$^+$ (adipocyte progenitor cells) cell populations are shown in each plot. (**B**) The percentage of Lin$^-$, CD24$^+$, CD34$^+$ and CD29$^+$ (adipocyte progenitor cells) is quantified at each time point. *n*=6 wounds from three mice for all time points. (**C**) The percentage of proliferative (BrdU$^+$) adipocyte progenitor cells increases during wound healing. *n*=6 wounds from three mice for all time points. Error bars indicate s.e.m. NW, non-wounded control.

bed in multiple mice, we determined the relative fluorescence intensity of ER-TR7 and α-SMA immunostaining in the wound bed (Fig. 3F). Wounds of AZIP mice showed a significant reduction in fluorescence intensity for ER-TR7 and α-SMA in the wound bed but not in the area adjacent to the wound. Overall, these defects suggest that the adipocytes are required for fibroblast presence in the wound bed following skin wounding.

Inhibition of PPARγ abrogates adipocyte repopulation of skin wounding

To further address the role of adipocytes in the skin during wounding, adipogenesis was inhibited in mice using two different PPARγ inhibitors: GW9662 and bisphenol A diglycidyl ether (BADGE) (Bendixen et al., 2001; Wright et al., 2000). Since keratinocytes and fibroblasts do not express PPARγ in wounded skin (Michalik et al., 2001), we did not anticipate that PPARγ inhibition would alter keratinocyte or fibroblast function. Indeed, mice treated with GW9662 did not display defects in keratinocyte proliferation or re-epithelialization (supplementary material Fig. S1B). Furthermore, fibroblasts treated *in vitro* with increasing concentrations of GW9662 migrated similarly to cells treated with vehicle (supplementary material Fig. S1A). Proliferation of primary fibroblasts was also unaffected, as determined by BrdU incorporation analysis by flow cytometry (supplementary material Fig. S1A). Therefore, GW9662 does not directly alter keratinocyte or primary fibroblast proliferation or migration.

Since PPARγ has been reported to regulate regenerative macrophage function (Chawla et al., 1994; Gautier et al., 2012), we analyzed the recruitment and function of immune cell populations in the wounds of GW9662-treated mice. Mice treated with GW9662 did not display defects in the percentage of CD45$^+$, CD11b$^+$ (ITGAM – Mouse Genome Informatics), F4/80$^+$ macrophages within the wounds at 3 days (supplementary material Fig. S2A). Immunostaining sections of 3-day wounds from vehicle- or GW9662-treated mice with antibodies against F4/80 and LY6G indicated normal recruitment of macrophages and neutrophils, respectively (supplementary material Fig. S2B). The normal recruitment of CD45$^+$ immune cells was further confirmed by FACS at 5 and 7 days after wounding in vehicle- and GW9662-treated wounds (supplementary material Fig. S2C). To analyze macrophage function in GW9662-treated wounds, we examined mRNA for cytokines known to be expressed by macrophages following wounding (Delavary et al., 2011; DiPietro, 1995). Macrophages from vehicle- and GW9662-treated mice expressed similar amounts of mRNA for the cytokines *Mmp9*, *Tgfb*, *Pdgfa* and *Il10* (supplementary material Fig. S2D). These data suggest that the general expression of these cytokines in macrophages is not altered with pharmacological inhibition of PPARγ during skin wounding.

To confirm that inhibition of PPARγ blocks adipogenesis of intradermal adipocytes during wound healing, we analyzed adipocyte regeneration in wounds of WT mice treated with GW9662 or BADGE by immunostaining with antibodies against perilipin. After 5 and 7 days, wounded skin from mice injected with GW9662 and BADGE exhibited a significant reduction in the number of adipocytes in the wound bed compared with vehicle-injected controls (supplementary material Fig. S3A), supporting the ability of GW9662 to block adipocyte maturation during wound healing.

To determine whether GW9662 affects the proliferation of adipocyte precursor cells *in vivo*, we pulsed mice with BrdU for 2 days during a wound healing timecourse in vehicle- and GW9662-treated mice and analyzed adipocyte precursor cells by flow cytometry. GW9662 treatment caused no difference in the proliferation of adipocyte precursors at either 5 or 7 days after wounding when compared with vehicle-injected controls. In addition, the number of adipocyte precursors in wounds was comparable to that of vehicle-injected controls (supplementary material Fig. S3C).

Inhibition of adipogenesis abrogates fibroblast repopulation of skin wounds

Next, we investigated whether GW9662-treated mice display defects in wound healing. Mice were treated with vehicle or GW9662 following full-thickness punch biopsies. Histological analysis of wounded skin of GW9662-treated mice by H&E staining illustrated defects in the dermis (supplementary material Fig. S3B),

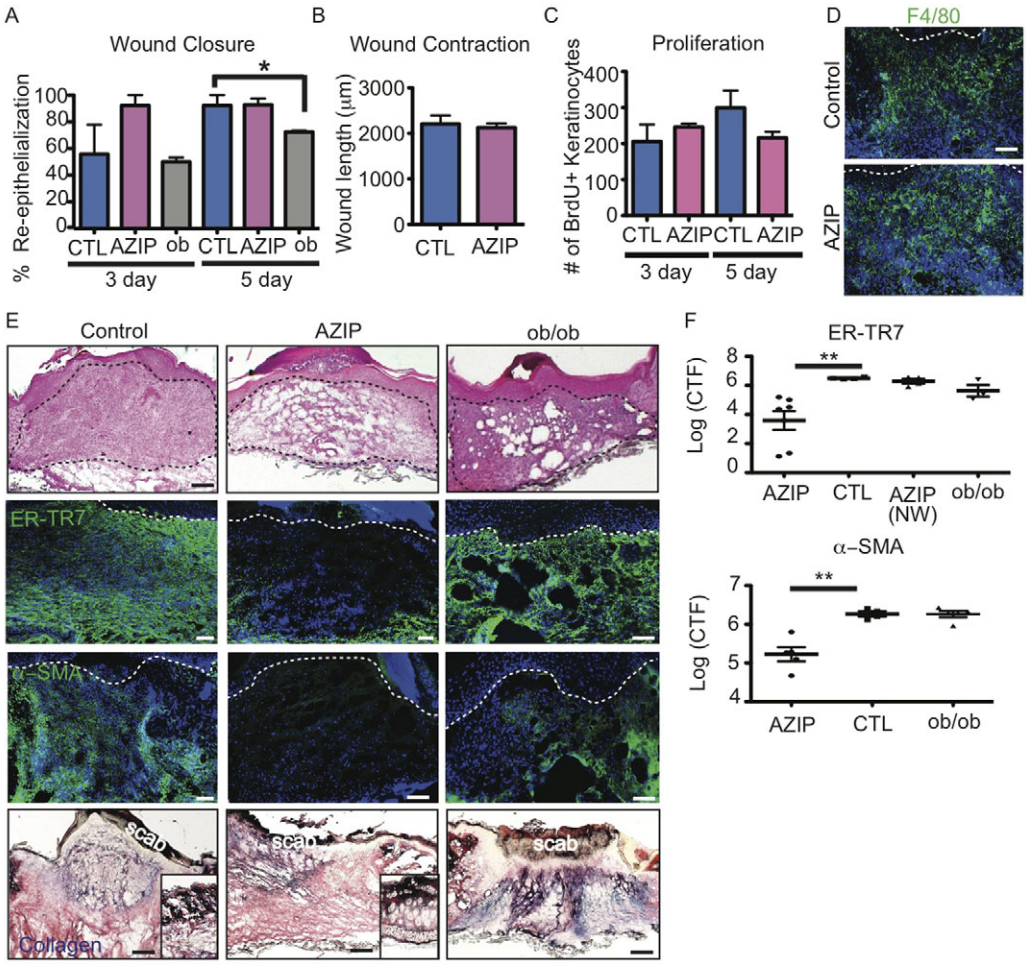

Fig. 3. AZIP skin wounds show dermal wound healing defects but normal re-epithelialization and macrophage recruitment. (**A**) The percentage of re-epithelialization is impaired in wounds of ob/ob mice at 5 days but not in wounds of AZIP mice as compared with wounds of littermate controls. **P*=0.03. *n*=2-4 wounds per mouse from three to five mice. (**B**) Wound contraction is determined by measuring the distance between the edges of the panniculus carnosus. There is no significant difference in AZIP mouse wounds compared with WT. *n*>6 wounds from four mice. (**C**) Proliferation of keratinocytes was measured by incorporation of BrdU after a 24-hour pulse. The number of BrdU$^+$ keratinocytes is similar in littermate control and AZIP wounds at 3 and 5 days. *n*=4 per mouse for three to five mice. (**D**) AZIP wounds show F4/80$^+$ macrophage populations similar to controls at 5 days after wounding. Dotted line indicates the epidermal-dermal boundary. (**E**) H&E-stained and immunostained sections of wounds from AZIP, ob/ob and FVB control mice 7 (AZIP, FVB) or 5 (ob/ob) days after wounding. The AZIP dermal compartment is noticeably disorganized compared with that of controls (black dotted line). Skin wounds of AZIP mice show a lack of ER-TR7$^+$ or α-SMA$^+$ dermal fibroblasts, whereas ob/ob mice display normal fibroblast presence. Trichrome staining (bottom row) shows a lack of collagen in the wound bed of AZIP mice compared with controls and ob/ob wounds, but normal collagen localization in non-wounded dermis (insets). White dotted line indicates epidermal-dermal boundary. (**F**) Corrected total fluorescence (CTF) of immunostaining with ER-TR7 and α-SMA antibodies in wound beds of 7-day wounds from mice of the indicated genotype. For each image, CTF was calculated by determining the integrated density of wound bed fluorescence or adjacent non-wounded area (NW) and subtracting the area multiplied by the mean background fluorescence of the epidermis. ***P*=0.009, ER-TR7; ***P*=0.005, α-SMA. *n*=8 wounds from four mice. Error bars indicate s.e.m. Scale bars: 100 μm, except 200 μm in E (top).

similar to defects following wounding in AZIP mice. Immunostaining with antibodies against ER-TR7 and α-SMA revealed that fibroblasts were absent within the wound bed but present adjacent to the wound in both GW9662- and BADGE-treated mice (Fig. 4A). Quantification of multiple experiments revealed a significant reduction in the fluorescence intensity of ER-TR7 and α-SMA staining in the wound bed of GW9662-treated mice but not in adjacent non-wounded areas (Fig. 4B). These data suggest that inhibition of adipocytes with PPARγ inhibitors results in dermal defects similar to those observed in AZIP mice.

To further analyze myofibroblast presence in wounds of vehicle- and GW9662-treated mice, we analyzed α-SMA$^+$ cells by flow cytometry. Isotype control antibodies confirmed the specificity of intracellular staining of α-SMA antibodies (supplementary material Fig. S3D). Whereas α-SMA$^+$ cells increased following wounding in vehicle-treated mice, α-SMA$^+$ cells were significantly reduced at day 7 following wound healing in mice treated with GW9662 (Fig. 4C). In addition, a population of CD45$^+$, α-SMA$^+$ cells, which have been suggested to be fibrocytes (Kao et al., 2011), was also significantly reduced at both 5 and 7 days after wounding in GW9662-treated mice compared with vehicle-treated controls. Reduction of α-SMA-expressing cells in 5-day wounds of GW9662-treated mice was confirmed by western blot analysis (Fig. 4D). These data support a reduction in

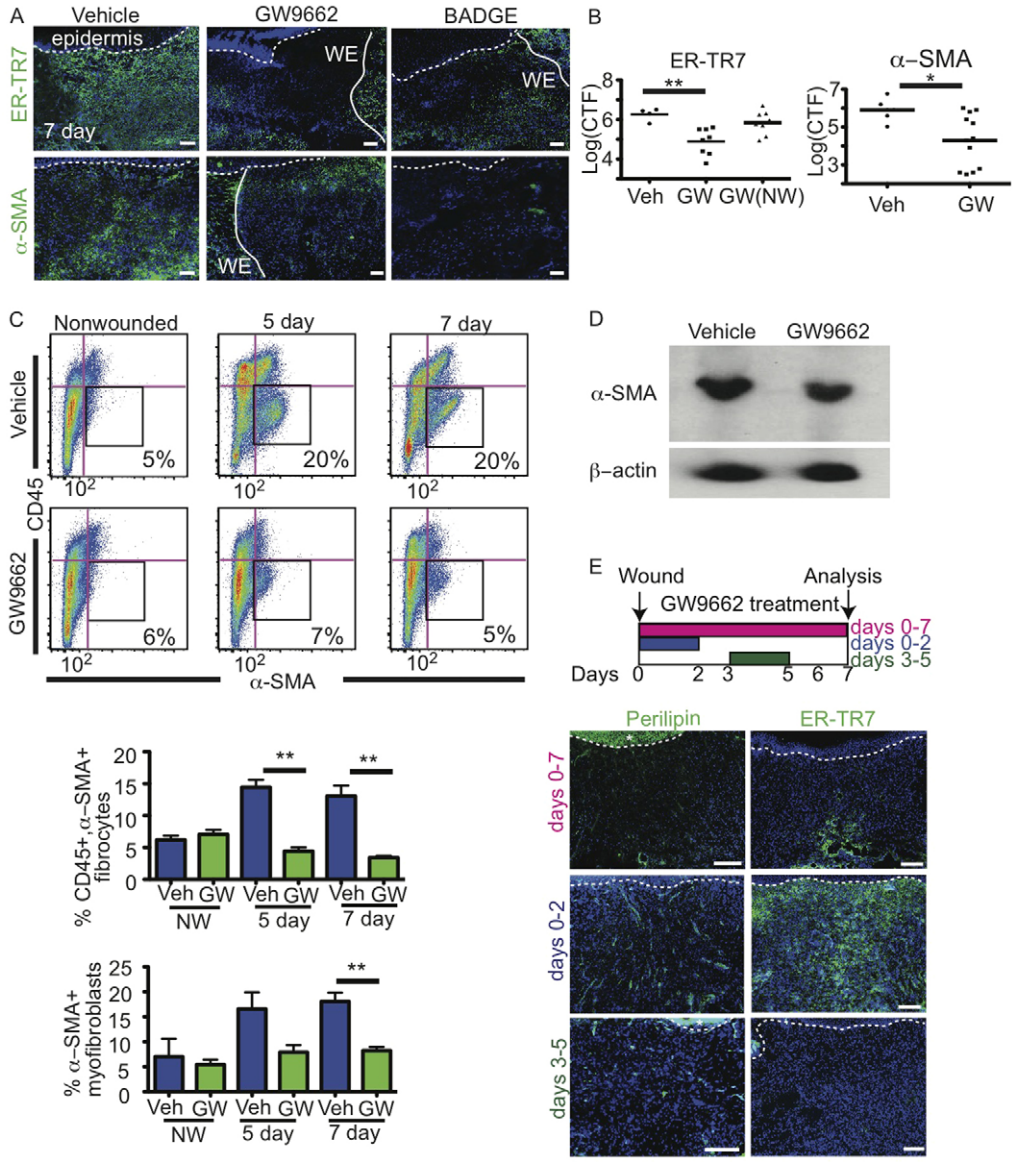

Fig. 4. Pharmacological inhibition of adipogenesis abrogates fibroblast presence in skin wounds. (**A**) ER-TR7$^+$ fibroblasts and α-SMA$^+$ myofibroblasts are absent in GW9662-injected and BADGE-injected wound beds compared with vehicle-injected controls at 7 days after wounding, but are present along wound edges (WE, solid line). Dotted line indicates epidermal-dermal boundary. (**B**) Corrected total fluorescence (CTF) of immunostaining with ER-TR7 and α-SMA antibodies in wound bed or non-wounded (NW) dermal regions of 5-day wounds of mice of the indicated genotype. n=10 wounds from five mice. $^{**}P$=0.004, ER-TR7; $^{*}P$=0.016, α-SMA. Veh, vehicle-treated control. (**C**) Dot plots with biexponential x-axes showing FACS staining and gating of CD45$^-$/α-SMA$^+$ myofibroblasts (black boxes) from non-wounded or wounded vehicle- and GW9662-injected mice at 5 and 7 days after wounding. Percentages of myofibroblasts are indicated in each plot. Beneath is shown the quantification of the CD45$^+$/α-SMA$^+$ fibrocytes and CD45$^-$/α-SMA$^+$ myofibroblasts in non-wounded, 5-day or 7-day wounds. $^{**}P$=0.007. n=6 mice for each time point from two experiments. (**D**) Western analysis confirms the decrease in α-SMA production in GW9662-injected mouse skin compared with the wounds of vehicle-injected controls at 5 days after wounding. (**E**) The experimental design to treat mice with GW9662 during different time points following wounding. Mice were treated with GW9662 from days 0-2, 3-5 or 0-7 and analyzed at day 7. Beneath is shown immunostaining with antibodies against perilipin, demonstrating reduced adipocyte formation with GW9662 treatment from days 3-5 or 0-7. Fibroblasts (ER-TR7$^+$ cells) are recruited into the wound bed when mice are treated with GW9662 from days 0-2 but impaired at other time points. Dotted line indicates epidermal-dermal boundary. Asterisk indicates background staining in epidermis. Error bars indicate s.e.m. Scale bars: 100 μm.

fibroblast function following wound healing in mice treated with PPARγ inhibitors.

To confirm that early events in wound healing were not inhibited by inhibition of PPARγ during wound healing, we injected mice with GW9662 from days 0-2 or 3-5 following wounding and analyzed the mice at day 7. Adipocytes were present in wounded skin when mice were treated with GW9662 from days 0-2 but were reduced in number with GW9662 injections on days 3-5 (Fig. 4E). Analysis of ER-TR7 expression revealed that fibroblasts were present in the wounds when GW9662 was injected in the first 2 days after wounding, but fibroblasts were absent from wounds when GW9662 was injected 3-5 days following wounding. These data confirm that inhibition of adipocyte formation during wound healing abrogates fibroblast presence in skin wounds and suggest

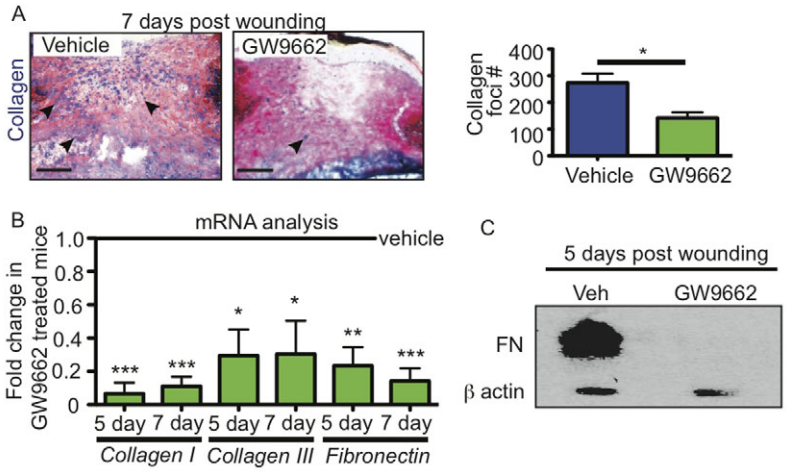

Fig. 5. PPARγ inhibitors influence fibroblast function during wound healing. (**A**) Collagen production is reduced in GW9662-injected wounds compared with vehicle controls as seen by trichrome staining. Arrowheads indicate collagen production. To the right is shown the quantitation of collagen foci in vehicle- and GW9662-injected mice at 7 days after wounding. **P*=0.0125. *n*=4-5 wounds from four mice. (**B**) mRNA analysis via real-time PCR of collagen Iα1, collagen IIIα1 and fibronectin in wounds of mice injected with GW9662 indicates reduced expression of these genes compared with wounds of vehicle-injected mice at the same time point after wounding. **P*>0.02, ***P*=0.003, ****P*=0.0001. *n*=6-8 wounds from two experiments for each time point. (**C**) Western analysis confirms the lack of fibronectin (FN) protein production in wounds of GW9662-injected mice compared with wounds of vehicle-injected mice 5 days after wounding. Error bars indicate s.e.m. Scale bars: 200 μm.

that GW9662 does not alter the function of non-adipocyte cell types during the earliest stages of wound healing.

To analyze fibroblast function during skin wound healing, we measured the expression of extracellular matrix (ECM) component mRNA and protein. The wound beds of GW9662-treated mice lacked trichrome staining of collagen foci, which were prevalent in the wounds of vehicle-treated mice at 7 days after wounding (Fig. 5A). The reduction in collagen within wounds of GW9662-treated mice was confirmed by real-time PCR (Fig. 5B). In addition, fibronectin mRNA and protein levels were significantly reduced in GW9662-treated mouse wounds, as determined by real-time PCR and western blot analyses, respectively (Fig. 5C). Taken together, these data suggest that adipocytes are required for fibroblast function during skin wound healing.

Defects in adipocyte function during wound healing result in wound failure

To determine whether fibroblast defects during wound healing due to a lack of adipocytes lead to skin failure and wound recurrence, we analyzed wounds of control, AZIP and GW9662-treated mice 2 weeks after punch biopsy. Histologically, the wounds of AZIP and GW9662-treated mice appeared more defective at 2 weeks than at 1 week (Fig. 6A). Despite the lack of defects in wound bed size after 1 week, the AZIP mice displayed a significantly larger wound bed area and wound length after 2 weeks, as compared with control mice at 2 weeks (Fig. 6B). Similarly, the wounds of mice treated with GW9662 for 2 weeks displayed a similar expansion in the size of the dermal compartment after 2 weeks (Fig. 6C).

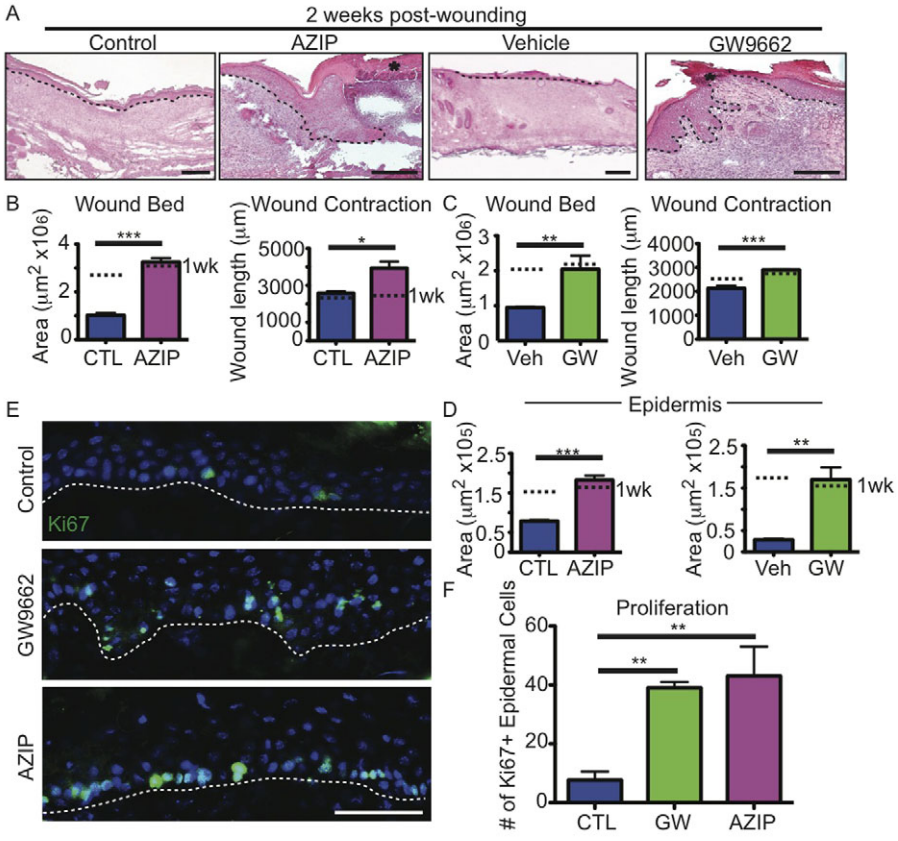

Fig. 6. Wound recurrence after 2 weeks of healing in AZIP and GW9662-treated mice. (**A**) H&E-stained sections illustrate the development of epidermal defects and a lack of dermal healing in AZIP and GW9662-injected mice 2 weeks after wounding. Dotted line indicates epidermal-dermal boundary. Asterisk indicates new scab over wound. (**B**,**C**) Wound bed area and wound contraction are significantly increased in AZIP and GW9662-injected (GW) mice compared with controls. **P*=0.02, ***P*=0.002-0.003, ****P*=0.0004-0.0008. *n*=3-4 wounds from four mice for each condition. Dotted lines indicate mean values at 1 week (wk). (**D**) Epidermal area is increased in AZIP and GW9662-injected wounds after 2 weeks. ***P*=0.002-0.005, ****P*=0.0008 *n*=3-4 wounds from three mice for each condition. (**E**) KI67 immunostaining of skin sections of control, AZIP and GW9662-injected mice 2 weeks after wounding. (**F**) Quantification of KI67^{+} cells in the epidermis of control, GW9662-injected and AZIP mice 2 weeks after wounding. ***P*=0.004-0.006. *n*=3 wounds from three mice for each condition. Error bars indicate s.e.m. Scale bars: 200 μm in A; 50 μm in E.

The wounds of AZIP and GW9662-treated mice also developed keratinocyte defects after 2 weeks, as indicated by an increase in the epidermal area of the wounds (Fig. 6A,D). This increase in epidermal area correlated with an increase in KI67$^+$ (MKI67 – Mouse Genome Informatics) keratinocytes in the wounded skin of AZIP and GW9662-treated mice compared with control wounds (Fig. 6E,F). In fact, 50% of AZIP and GW9662-treated wounds re-opened, as indicated by a lack of a continuous epidermis over the wound bed (Fig. 6A). These data demonstrate that the dermal defects that occur in the absence of adipocytes lead to defects in dermal remodeling that compromise the integrity of the closed wounds, resulting in skin failure and wound recurrence.

Adipocytes may promote fibroblast production and migration during skin wound healing

Adipocytes may influence fibroblast function during skin wound healing by altering fibroblast development from a precursor cell, the expansion of resident fibroblasts via proliferation, and/or the migration of fibroblasts into the wound. To determine whether fibroblast production is altered in the absence of adipocytes, we quantified the number of ER-TR7$^+$ fibroblasts in AZIP and GW9662-treated mice after wounding (Fig. 7A). Consistent with our previous results, fewer fibroblasts were found within wounds of AZIP and GW9662-treated mice. Examination of the number of ER-TR7$^+$ cells outside the wound edge revealed that AZIP and GW9662-treated mice have a similar or increased number of fibroblasts compared with control wounds outside of the wound bed. The total number of fibroblasts is significantly decreased in the absence of adipocytes in both AZIP mice at 7 days and GW9662-treated mice at 5 days, but the difference in fibroblast number does not persist in GW9662-treated mice at 7 days.

To determine whether defects in fibroblast proliferation occur in the absence of adipocyte formation, we pulsed wounded vehicle- or GW9662-treated mice with BrdU for 48 hours and analyzed day-5 wounds. We stained skin sections from GW9662-injected mice and controls with antibodies against BrdU and vimentin, an intermediate filament protein that is expressed in fibroblasts (Chang et. al., 2002) (Fig. 7B). Five days after wounding, the same number of vimentin$^+$ cells at the edge of the wound bed are proliferative in vehicle- and GW9662-injected mice (Fig. 7B), suggesting that fibroblast proliferation is not altered in the absence of adipocytes. Taken together with the reduction in fibroblasts in AZIP and

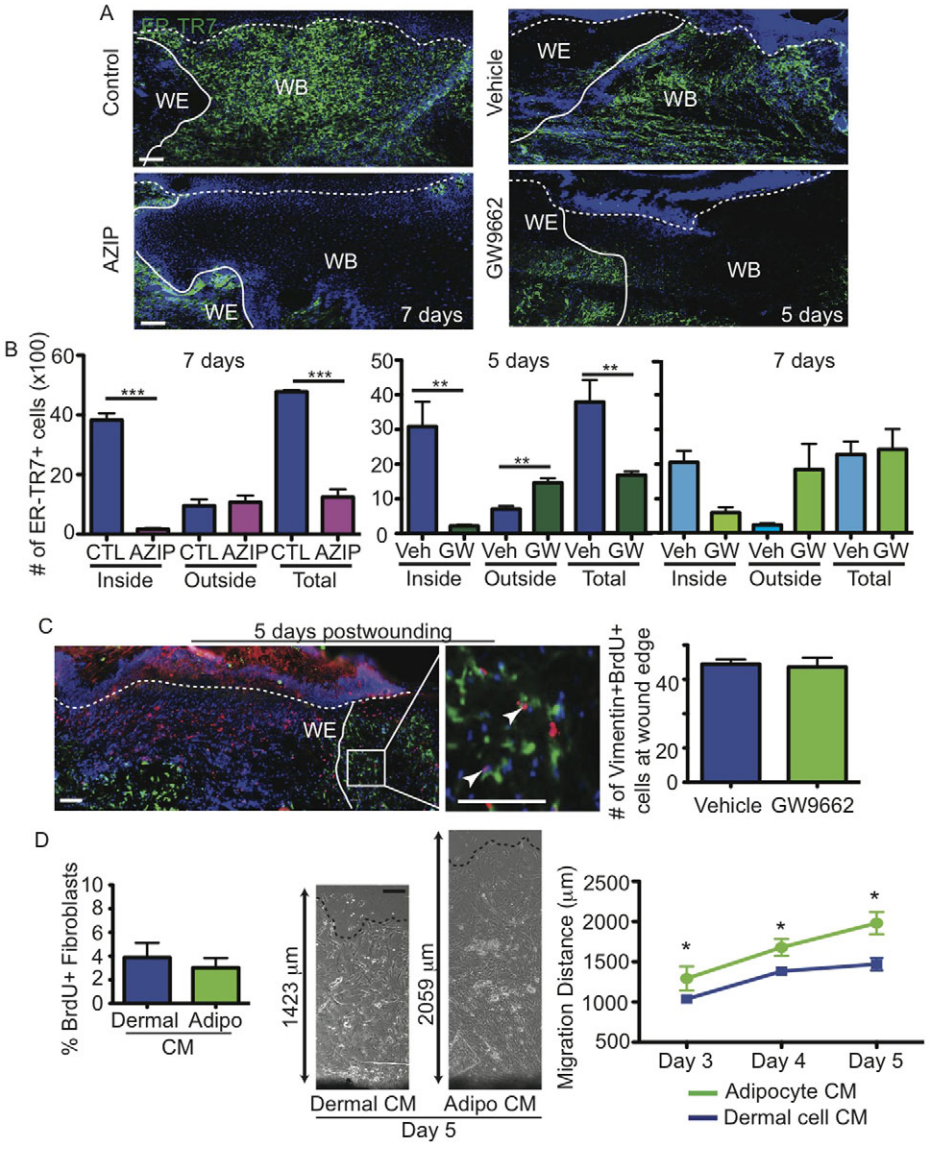

Fig. 7. Adipocytes influence fibroblast migration and not proliferation. (**A**) Skin sections immunostained with ER-TR7 antibodies illustrate the location of fibroblasts at the wound edge (WE, solid line) in AZIP and GW9662-treated mice and in the wound bed (WB) in control mice at the indicated days after wounding. Dotted line represents epidermal-dermal boundary. (**B**) The number of ER-TR7$^+$ fibroblasts in the entire wound was quantified in high-magnification images of immunostained skin sections from control (CTL), AZIP, vehicle- and GW9662-treated mice at the indicated days after wounding. $^{**}P$=0.005-0.008, $^{***}P$=0.0001-0.0002. n=3 wounds from three mice for each genotype or condition. (**C**) Analysis of fibroblast proliferation by immunostaining with antibodies against vimentin (green) and BrdU (red). Arrowheads indicate proliferating fibroblasts. To the right is shown the quantification of vimentin$^+$, BrdU$^+$ fibroblasts at the wound edge in vehicle- and GW9662-injected mice, demonstrating no difference in proliferative cell number. n=7 wounds from three mice for each condition. (**D**) Analysis of fibroblast proliferation and migration from skin explants in dermal cell- or adipocyte (Adipo)-conditioned medium (CM). Fibroblasts in dermal cell- or adipocyte cell-conditioned medium were analyzed for BrdU incorporation during a 6-hour pulse. Phase-contrast images are shown of skin explants (black, bottom), illustrating the difference in migration distance. Fibroblast outgrowth is enhanced in skin explants in adipocyte-conditioned medium compared with dermal cell-conditioned medium. $^*P$=0.04-0.01. n=3 explants in two independent experiments. Error bars indicate s.e.m. Scale bars: 100 µm.

GW9662-treated mice, these data suggest that alterations in adipocyte formation can hinder the production of fibroblasts, which might occur by influencing the activity of an unidentified fibroblast precursor cell.

Since fibroblasts are present outside the wound edge of AZIP and GW9662-treated mice but do not seem to migrate into the wound bed, we sought to determine if adipocytes secrete factors that promote fibroblast migration. We determined whether adipocyte-conditioned media could influence primary fibroblast migration from explants of skin. Primary dermal cells or adipocytes from FACS-purified skin cells were plated in fibroblast medium, and conditioned medium was collected after mature adipocytes had formed in cultures of adipocyte lineage cells (Festa et al., 2011). Addition of adipocyte-conditioned medium to explants of tail skin did not induce fibroblast proliferation but enhanced fibroblast migration from the edge of the skin explant when compared with the addition of conditioned medium from total dermal cells (Fig. 7C). These data suggest that adipocytes might promote fibroblast production from precursor cells and/or enhance fibroblast migration into the wound bed so as to mediate fibroblast recruitment during skin wound healing.

DISCUSSION

Adipocytes repopulate skin wounds during the proliferative phase of healing

Our data show that the proliferative phase of wound healing involves the repopulation of adipocytes within skin wounds. We show that immature adipocytes are activated during the proliferative phase of acute skin wound healing and mature, perilipin^{+} adipocytes and fibroblasts appear in healing wounds concurrently. The lack of adipocytes in the wounds of mice treated with PPARγ inhibitors suggests that the repopulation of adipocytes during wounding occurs via adipogenesis. Adipocyte migration from non-wounded areas might also contribute to the repopulation of adipocytes within skin wounds.

Our data indicate that the activation of adipocyte precursor cells following wounding occurs after immune cells infiltrate the wound bed and concurrently with fibroblast migration. The activation of adipocyte precursors and their differentiation into mature adipocytes may be promoted by immune cells in the wound bed. An interplay between hematopoietic and adipocyte lineage cells has been shown *in vitro*. Macrophages can stimulate preadipocyte proliferation (Keophiphath et al., 2009; Chazenbalk et al., 2011) and induce alterations in cell morphology by modulating actin cytoskeletal organization and focal adhesions (Keophiphath et al., 2009). Accumulation of macrophages and immune cells in adipose tissue is enhanced in obesity, leading to increased inflammation and cytokine production (Lumeng et al., 2007; Kintscher et al., 2008). Although the specific nature of these signals remains elusive, it is possible that adipocyte lineage cells are responding to molecules secreted by macrophages or other immune cell types in wounded tissue, leading to adipogenesis.

Wound healing defects in mice lacking adipocytes support the existence of two distinct but interdependent stages of the proliferative phase of skin wounding: an initial keratinocyte-mediated phase that seals the epithelial barrier, followed by a fibroblast-mediated phase that remodels the dermis to maintain epithelial structure and requires proper adipogenesis. Wounds in both AZIP mice and mice treated with PPARγ inhibitors lack mature adipocytes and display abrogated fibroblast presence and deposition of ECM proteins into the wound bed. However, keratinocyte re-epithelialization and wound contraction were not aberrant in these mouse models during the first week of healing, and thus do not seem to depend on the presence of fibroblasts in the wound bed. Keratinocytes are known to respond to cytokines produced by immune cells (Hübner et al., 1996) and might not require additional signals from fibroblasts to initially close the epithelial barrier. Furthermore, in the wounding paradigm used in this study, wound contraction after 1 week occurred in the absence of mature adipocytes, suggesting that myofibroblasts at the edge of wounds might be sufficient for initial wound contraction. However, the absence of fibroblasts and dermal remodeling in the absence of adipocytes led to a failure of the epithelium after 2 weeks, suggesting that adipocytes promote dermal remodeling to generate a robust structure to maintain the skin epithelium.

Direct or indirect communication may exist between adipocytes and fibroblasts

Given the reduction in fibroblasts in mice with defects in adipogenesis, adipocytes might indirectly contribute to fibroblast recruitment by controlling the production of an unidentified fibroblast precursor cell in the skin. During skeletal muscle regeneration, fibroblasts and adipocytes can derive from a common fibro/adipogenic progenitor (Joe et al., 2010; Uezumi et al., 2011). Another fibroblast-like cell type that might be in a shared lineage relationship with skin adipocyte lineage cells are the fibrocytes, which are immature fibroblast-like cells that play significant roles in tissue remodeling during skin wound healing (Bucala et al., 1994; Chesney et al., 1998) and have the capacity to differentiate into adipocytes in a PPARγ-dependent manner (Hong et al., 2005). Since mature adipocytes and fibroblasts appear in the wound bed simultaneously, a common precursor might be activated and differentiate into fibroblast and adipocyte progeny. This possibility is supported by the ability of skin-derived precursors to repopulate multiple cell lineages within the dermis, including fibroblasts and adipocytes (Biernaskie et al., 2009). Alternatively, adipocytes and fibroblasts might have distinct precursor cells resident in the skin that become activated concurrently. Additional characterization of fibroblast populations in the skin and how they are altered in mice lacking adipocyte lineage cells will define how these cell types contribute to the production of adipocytes and fibroblasts in the skin.

In addition, our data implicate a direct intercellular communication between adipocytes and fibroblasts that might contribute to fibroblast migration during dermal healing of skin wounds. In the skin, mature adipocytes produce platelet-derived growth factor (PDGF) ligands (Blanpain et al., 2004; Festa et al., 2011) and bone morphogenetic proteins (BMPs) (Plikus et al., 2008), both of which have been suggested to regulate wound healing processes. PDGF has many important roles in skin wound healing and serves as a chemotactic agent for neutrophils, macrophages and fibroblasts (Heldin and Westermark, 1999). The primary source of PDGF in healing skin wounds is thought to be platelets (Vogt et al., 1998), but adipocytes may contribute to later PDGF expression in skin wounds. The role of BMPs in skin wounding has not been explored extensively. Addition of BMP2 in fetal wounds can increase fibroblast recruitment (Stelnicki et al., 1998), suggesting that BMP expression by mature adipocytes might mediate the function of adipocytes during wounding. In other adipocyte depots, mature adipocytes generate adipokines, such as adiponectin, leptin and free fatty acids, which can signal to other tissues and influence metabolism (Sumida et al., 1993; Ouchi et al., 2011; Rosen and Spiegelman, 2006). Our future studies will explore the molecular mechanisms that underlie adipocyte function during wound healing in the skin.

Diabetes may influence fibroblast function during skin wound healing

Our results reveal that distinct wound healing defects occur in two diabetic mouse models. The genetically obese (ob/ob) mice have been used extensively to study the effects of diabetes on skin wound healing because they display severe defects in re-epithelialization similar to chronic wounding in diabetic patients (Frank et al., 2000; Werner et al., 1994; Mustoe, 2004). These impairments have been attributed to the lack of growth factors important for proper keratinocyte, endothelial cell and fibroblast function due to an increase in local inflammatory responses (Wetzler et al., 2000; Goren et al., 2003; Taylor et al., 2011). Interestingly, despite the diabetic phenotype in AZIP mice, we did not observe an increase in the inflammatory response or defects in re-epithelialization in wounds, suggesting that the diabetic phenotype might be distinct in these mice. Several characteristics of diabetes are shared between ob/ob and AZIP mice, such as increased glucocorticoid levels and insulin resistance. However, differences in the regulation of glucose homeostasis might allow AZIP mice to elicit a proper immune response and re-epithelialize their wounds.

It is interesting to note that human patients with diabetes or who suffer from malnutrition have impaired skin wound healing. The absence of nutrients, such as fatty acids, in the skin can lead to altered cell proliferation and maintenance and decreased ECM production, ultimately contributing to non-healing skin conditions such as ulcers (Arnold and Barbul, 2006; Brown and Phillips, 2010). By defining the role of adipocyte lineage cells in the skin, we have identified that these cells dynamically promote skin wound healing. It will be important for future studies to determine whether adipocytes can aid healing in chronic wounding or ameliorate fibrotic diseases, and to uncover the mechanisms by which they do so.

Acknowledgements

We thank Tudorita Tumbar, Michael Rendl, Hoang Ngyuen, Matthew Rodeheffer, Ryan Berry and V.H. laboratory members for technical assistance, critical reading of the manuscript and valuable discussions.

Funding

V.H. is a Pew Scholar in Biomedical Research and is funded by the National Institutes of Health (AR060295) and CT Innovations [12-SCB-YALE-01]. Deposited in PMC for release after 12 months.

Competing interests statement

The authors declare no competing financial interests.

Supplementary material

Supplementary material available online at
http://dev.biologists.org/lookup/suppl/doi:10.1242/dev.087593/-/DC1

References

Arnold, M. and Barbul, A. (2006). Nutrition and wound healing. *Plast. Reconstr. Surg.* **117 Suppl.**, 42S-58S.

Bendixen, A. C., Shevde, N. K., Dienger, K. M., Willson, T. M., Funk, C. D. and Pike, J. W. (2001). IL-4 inhibits osteoclast formation through a direct action on osteoclast precursors via peroxisome proliferator-activated receptor gamma 1. *Proc. Natl. Acad. Sci. USA* **98**, 2443-2448.

Biernaskie, J., Paris, M., Morozova, O., Fagan, B. M., Marra, M., Pevny, L. and Miller, F. D. (2009). SKPs derive from hair follicle precursors and exhibit properties of adult dermal stem cells. *Cell Stem Cell* **5**, 610-623.

Blanpain, C., Lowry, W. E., Geoghegan, A., Polak, L. and Fuchs, E. (2004). Self-renewal, multipotency, and the existence of two cell populations within an epithelial stem cell niche. *Cell* **118**, 635-648.

Brack, A. S., Conboy, M. J., Roy, S., Lee, M., Kuo, C. J., Keller, C. and Rando, T. A. (2007). Increased Wnt signaling during aging alters muscle stem cell fate and increases fibrosis. *Science* **317**, 807-810.

Brown, K. L. and Phillips, T. J. (2010). Nutrition and wound healing. *Clin. Dermatol.* **28**, 432-439.

Bucala, R., Spiegel, L. A., Chesney, J., Hogan, M. and Cerami, A. (1994). Circulating fibrocytes define a new leukocyte subpopulation that mediates tissue repair. *Mol. Med.* **1**, 71-81.

Campfield, L. A., Smith, F. J., Guisez, Y., Devos, R. and Burn, P. (1995). Recombinant mouse OB protein: evidence for a peripheral signal linking adiposity and central neural networks. *Science* **269**, 546-549.

Chang, H. Y., Chi, J. T., Dudoit, S., Bondre, C., van de Rijn, M., Botstein, D. and Brown, P. O. (2002). Diversity, topographic differentiation, and positional memory in human fibroblasts. *Proc. Natl. Acad. Sci. USA* **99**, 12877-12882.

Chawla, A., Schwarz, E. J., Dimaculangan, D. D. and Lazar, M. A. (1994). Peroxisome proliferator-activated receptor (PPAR) gamma: adipose-predominant expression and induction early in adipocyte differentiation. *Endocrinology* **135**, 798-800.

Chazenbalk, G., Bertolotto, C., Heneidi, S., Jumabay, M., Trivax, B., Aronowitz, J., Yoshimura, K., Simmons, C. F., Dumesic, D. A. and Azziz, R. (2011). Novel pathway of adipogenesis through cross-talk between adipose tissue macrophages, adipose stem cells and adipocytes: evidence of cell plasticity. *PLoS ONE* **6**, e17834.

Chesney, J., Metz, C., Stavitsky, A. B., Bacher, M. and Bucala, R. (1998). Regulated production of type I collagen and inflammatory cytokines by peripheral blood fibrocytes. *J. Immunol.* **160**, 419-425.

Chua, S. C., Jr, Chung, W. K., Wu-Peng, X. S., Zhang, Y., Liu, S. M., Tartaglia, L. and Leibel, R. L. (1996). Phenotypes of mouse diabetes and rat fatty due to mutations in the OB (leptin) receptor. *Science* **271**, 994-996.

Delavary, B. M., van der Veer, W. M., Egmond, M. V., Niessen, F. B. and Beelen, R. H. J. (2011). Macrophages in skin injury and repair. *Immunobiology* **216**, 753-762.

DiPietro, L. A. (1995). Wound healing: the role of the macrophage and other immune cells. *Shock* **4**, 233-240.

Eguchi, J., Wang, X., Yu, S., Kershaw, E. E., Chiu, P. C., Dushay, J., Estall, J. L., Klein, U., Maratos-Flier, E. and Rosen, E. D. (2011). Transcriptional control of adipose lipid handling by IRF4. *Cell Metab.* **13**, 249-259.

Festa, E., Fretz, J., Berry, R., Schmidt, B., Rodeheffer, M., Horowitz, M. and Horsley, V. (2011). Adipocyte lineage cells contribute to the skin stem cell niche to drive hair cycling. *Cell* **146**, 761-771.

Frank, S., Stallmeyer, B., Kämpfer, H., Kolb, N. and Pfeilschifter, J. (2000). Leptin enhances wound re-epithelialization and constitutes a direct function of leptin in skin repair. *J. Clin. Invest.* **106**, 501-509.

Gautier, E. L., Chow, A., Spanbroek, R., Marcelin, G., Greter, M., Jakubzick, C., Bogunovic, M., Leboeuf, M., van Rooijen, N., Habenicht, A. J. et al. (2012). Systemic analysis of PPARγ in mouse macrophage populations reveals marked diversity in expression with critical roles in resolution of inflammation and airway immunity. *J. Immunol.* **189**, 2614-2624.

Gavet, O. and Pines, J. (2010). Progressive activation of CyclinB1-Cdk1 coordinates entry to mitosis. *Dev. Cell* **18**, 533-543.

Goren, I., Kämpfer, H., Podda, M., Pfeilschifter, J. and Frank, S. (2003). Leptin and wound inflammation in diabetic ob/ob mice: differential regulation of neutrophil and macrophage influx and a potential role for the scab as a sink for inflammatory cells and mediators. *Diabetes* **52**, 2821-2832.

Greenberg, A. S., Egan, J. J., Wek, S. A., Garty, N. B., Blanchette-Mackie, E. J. and Londos, C. (1991). Perilipin, a major hormonally regulated adipocyte-specific phosphoprotein associated with the periphery of lipid storage droplets. *J. Biol. Chem.* **266**, 11341-11346.

Heldin, C. H. and Westermark, B. (1999). Mechanism of action and in vivo role of platelet-derived growth factor. *Physiol. Rev.* **79**, 1283-1316.

Hong, K. M., Burdick, M. D., Phillips, R. J., Heber, D. and Strieter, R. M. (2005). Characterization of human fibrocytes as circulating adipocyte progenitors and the formation of human adipose tissue in SCID mice. *FASEB J.* **19**, 2029-2031.

Hubner G., Brauchle M., Rauchle M., Smola H., Madlener M. and Fassler R. (1996). Differential regulation of pro-inflammatory cytokines during wound healing in normal and glucocorticoid-treated mice. *Cytokine* **8**, 548-556.

Ingalls, A. M., Dickie, M. M. and Snell, G. D. (1950). Obese, a new mutation in the house mouse. *J. Hered.* **41**, 317-318.

Joe, A. W. B., Yi, L., Natarajan, A., Le Grand, F., So, L., Wang, J., Rudnicki, M. A. and Rossi, F. M. V. (2010). Muscle injury activates resident fibro/adipogenic progenitors that facilitate myogenesis. *Nat. Cell Biol.* **12**, 153-163.

Kao, H.-K., Chen, B., Murphy, G. F., Li, Q., Orgill, D. P. and Guo, L. (2011). Peripheral blood fibrocytes: enhancement of wound healing by cell proliferation, re-epithelialization, contraction, and angiogenesis. *Ann. Surg.* **254**, 1066-1074.

Keophiphath, M., Achard, V., Henegar, C., Rouault, C., Clément, K. and Lacasa, D. (2009). Macrophage-secreted factors promote a profibrotic phenotype in human preadipocytes. *Mol. Endocrinol.* **23**, 11-24.

Kilroy, G. E., Foster, S. J., Wu, X., Ruiz, J., Sherwood, S., Heifetz, A., Ludlow, J. W., Stricker, D. M., Potiny, S., Green, P. et al. (2007). Cytokine profile of human adipose-derived stem cells: expression of angiogenic, hematopoietic, and pro-inflammatory factors. *J. Cell. Physiol.* **212**, 702-709.

Kintscher, U., Hartge, M., Hess, K., Foryst-Ludwig, A., Clemenz, M., Wabitsch, M., Fischer-Posovszky, P., Barth, T. F. E., Dragun, D., Skurk, T. et al. (2008). T-lymphocyte infiltration in visceral adipose tissue: a primary event

in adipose tissue inflammation and the development of obesity-mediated insulin resistance. *Arterioscler. Thromb. Vasc. Biol.* **28**, 1304-1310.
Leibovich, S. J. and Ross, R. (1975). The role of the macrophage in wound repair. A study with hydrocortisone and antimacrophage serum. *Am. J. Pathol.* **78**, 71-100.
Lumeng, C. N., Bodzin, J. L. and Saltiel, A. R. (2007). Obesity induces a phenotypic switch in adipose tissue macrophage polarization. *J. Clin. Invest.* **117**, 175-184.
Mayer, J. and Barrnett, R. J. (1953). Sensitivity to cold in the hereditary obese-hyperglycemic syndrome of mice. *Yale J. Biol. Med.* **26**, 38-45.
Michalik, L., Desvergne, B., Tan, N. S., Basu-Modak, S., Escher, P., Rieusset, J., Peters, J. M., Kaya, G., Gonzalez, F. J., Zakany, J. et al. (2001). Impaired skin wound healing in peroxisome proliferator-activated receptor (PPAR)alpha and PPARbeta mutant mice. *J. Cell Biol.* **154**, 799-814.
Moitra, J., Mason, M. M., Olive, M., Krylov, D., Gavrilova, O., Marcus-Samuels, B., Feigenbaum, L., Lee, E., Aoyama, T., Eckhaus, M. et al. (1998). Life without white fat: a transgenic mouse. *Genes Dev.* **12**, 3168-3181.
Mustoe, T. (2004). Understanding chronic wounds: a unifying hypothesis on their pathogenesis and implications for therapy. *Am. J. Surg.* **187 Suppl. 1**, S65-S70.
Muzumdar, M. D., Tasic, B., Miyamichi, K., Li, L. and Luo, L. (2007). A global double-fluorescent Cre reporter mouse. *Genesis* **45**, 593-605.
Ouchi, N., Parker, J. L., Lugus, J. J. and Walsh, K. (2011). Adipokines in inflammation and metabolic disease. *Nat. Rev. Immunol.* **11**, 85-97.
Plikus, M. V., Mayer, J. A., de la Cruz, D., Baker, R. E., Maini, P. K., Maxson, R. and Chuong, C. M. (2008). Cyclic dermal BMP signalling regulates stem cell activation during hair regeneration. *Nature* **451**, 340-344.
Rodeheffer, M. S., Birsoy, K. and Friedman, J. M. (2008). Identification of white adipocyte progenitor cells in vivo. *Cell* **135**, 240-249.
Rosen, E. D. and Spiegelman, B. M. (2006). Adipocytes as regulators of energy balance and glucose homeostasis. *Nature* **444**, 847-853.
Ross, R. and Odland, G. (1968). Human wound repair. II. Inflammatory cells, epithelial-mesenchymal interrelations, and fibrogenesis. *J. Cell Biol.* **39**, 152-168.
Simpson, D. M. and Ross, R. (1972). The neutrophilic leukocyte in wound repair a study with antineutrophil serum. *J. Clin. Invest.* **51**, 2009-2023.
Stelnicki, E. J., Longaker, M. T., Holmes, D., Vanderwall, K., Harrison, M. R., Largman, C. and Hoffman, W. Y. (1998). Bone morphogenetic protein-2 induces scar formation and skin maturation in the second trimester fetus. *Plast. Reconstr. Surg.* **101**, 12-19.
Sumida, C., Graber, R. and Nunez, E. (1993). Role of fatty acids in signal transduction: modulators and messengers. *Prostaglandins Leukot. Essent. Fatty Acids* **48**, 117-122.
Sunderkötter, C., Steinbrink, K., Goebeler, M., Bhardwaj, R. and Sorg, C. (1994). Macrophages and angiogenesis. *J. Leukoc. Biol.* **55**, 410-422.
Taylor, K. R., Costanzo, A. E. and Jameson, J. M. (2011). Dysfunctional γδ T cells contribute to impaired keratinocyte homeostasis in mouse models of obesity. *J. Invest. Dermatol.* **131**, 2409-2418.
Uezumi, A., Ito, T., Morikawa, D., Shimizu, N., Yoneda, T., Segawa, M., Yamaguchi, M., Ogawa, R., Matev, M. M., Miyagoe-Suzuki, Y. et al. (2011). Fibrosis and adipogenesis originate from a common mesenchymal progenitor in skeletal muscle. *J. Cell Sci.* **124**, 3654-3664.
Vogt, P. M., Lehnhardt, M., Wagner, D., Jansen, V., Krieg, M. and Steinau, H. U. (1998). Determination of endogenous growth factors in human wound fluid: temporal presence and profiles of secretion. *Plast. Reconstr. Surg.* **102**, 117-123.
Werner, S., Breeden, M., Hübner, G., Greenhalgh, D. G. and Longaker, M. T. (1994). Induction of keratinocyte growth factor expression is reduced and delayed during wound healing in the genetically diabetic mouse. *J. Invest. Dermatol.* **103**, 469-473.
Wetzler, C., Kämpfer, H., Stallmeyer, B., Pfeilschifter, J. and Frank, S. (2000). Large and sustained induction of chemokines during impaired wound healing in the genetically diabetic mouse: prolonged persistence of neutrophils and macrophages during the late phase of repair. *J. Invest. Dermatol.* **115**, 245-253.
Wright, H. M., Clish, C. B., Mikami, T., Hauser, S., Yanagi, K., Hiramatsu, R., Serhan, C. N. and Spiegelman, B. M. (2000). A synthetic antagonist for the peroxisome proliferator-activated receptor gamma inhibits adipocyte differentiation. *J. Biol. Chem.* **275**, 1873-1877.
Wu, L., Yu, Y. L., Galiano, R. D., Roth, S. I. and Mustoe, T. A. (1997). Macrophage colony-stimulating factor accelerates wound healing and upregulates TGF-beta1 mRNA levels through tissue macrophages. *J. Surg. Res.* **72**, 162-169.
Zhang, Y., Proenca, R., Maffei, M., Barone, M., Leopold, L. and Friedman, J. M. (1994). Positional cloning of the mouse obese gene and its human homologue. *Nature* **372**, 425-432.

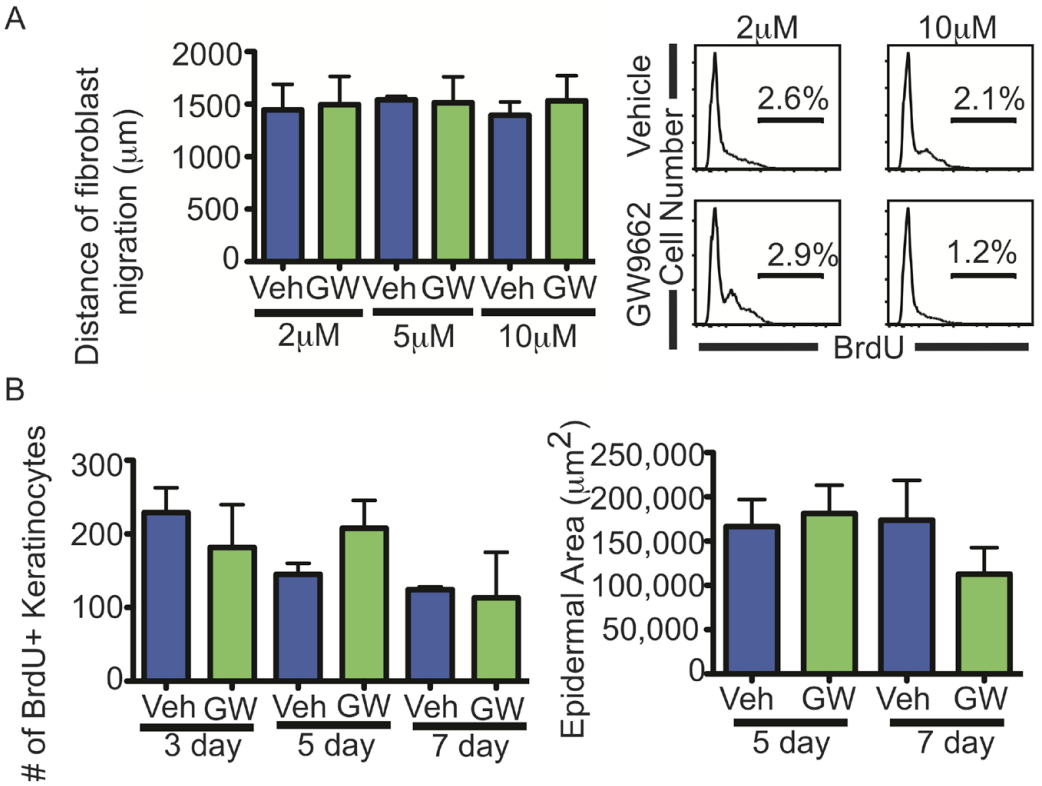

Fig. S1. GW9662 treatment does not directly affect fibroblasts *in vitro* or keratinocytes *in vivo*. (**A**) *In vitro* analysis of primary fibroblasts shows that fibroblast proliferation and migration are the same when cultured with vehicle or GW9662 at the indicated concentrations. (**B**) The number of $BrdU^+$ keratinocytes is the same in GW9662-injected mouse wounds and vehicle-injected controls at 3, 5 or 7 days after wounding. Additionally, the epidermal area is unchanged following GW9662 injection, indicating normal re-epithelialization.

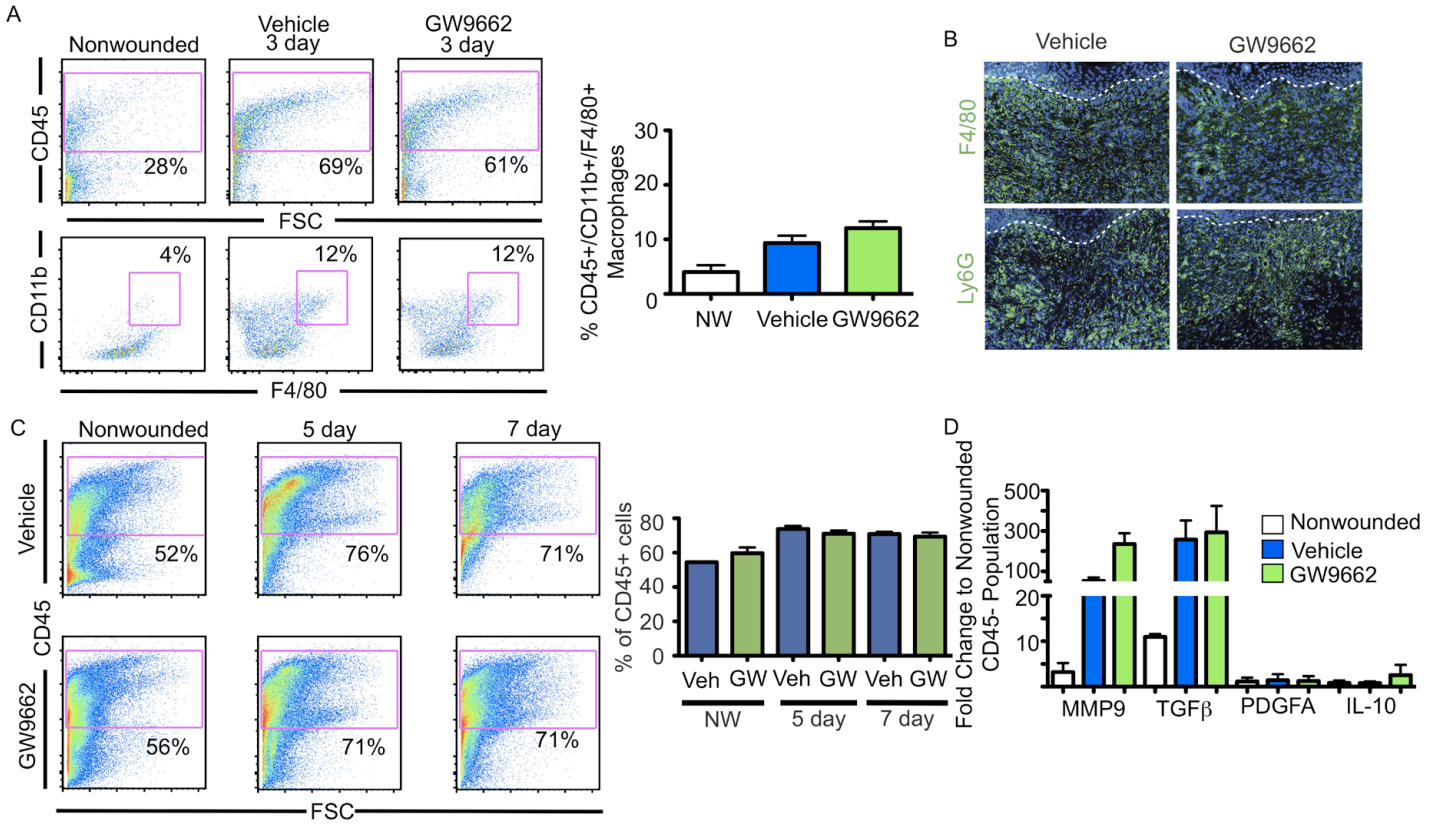

Fig. S2. Analysis of macrophages in GW9662-treated mice after wounding. (**A**) FACS analysis of $CD45^+/CD11b^+/F4/80^+$ macrophages at 3 days after wounding. Percentage of $CD45^+/CD11b^+/F4/80^+$ cells is similar in vehicle-injected and GW9662-injected mouse wounds. (**B**) Immune cell populations are recruited in GW9662-injected wounds compared with vehicle controls at 3 days after wounding. Macrophage populations can be seen in skin sections of both wounds using F4/80, and neutrophils infiltrate wounded skin normally in both samples as seen by LY6G immunostaining. Dotted lines indicate the epidermal-dermal boundary. Asterisk indicates background staining in epidermis. (**C**) FACS analysis of $CD45^+$ cells shows no difference in immune cell percentage of vehicle- and GW9662-injected mouse wounds at 5 or 7 days after wounding. (**D**) Fold changes of mRNA levels of $CD45^+/CD11b^+/F4/80^+$ macrophages compared with non-wounded $CD45^-$ controls isolated from non-wounded skin, vehicle-injected wounds and GW9662-injected wounds are similar for several macrophage-produced cytokines.

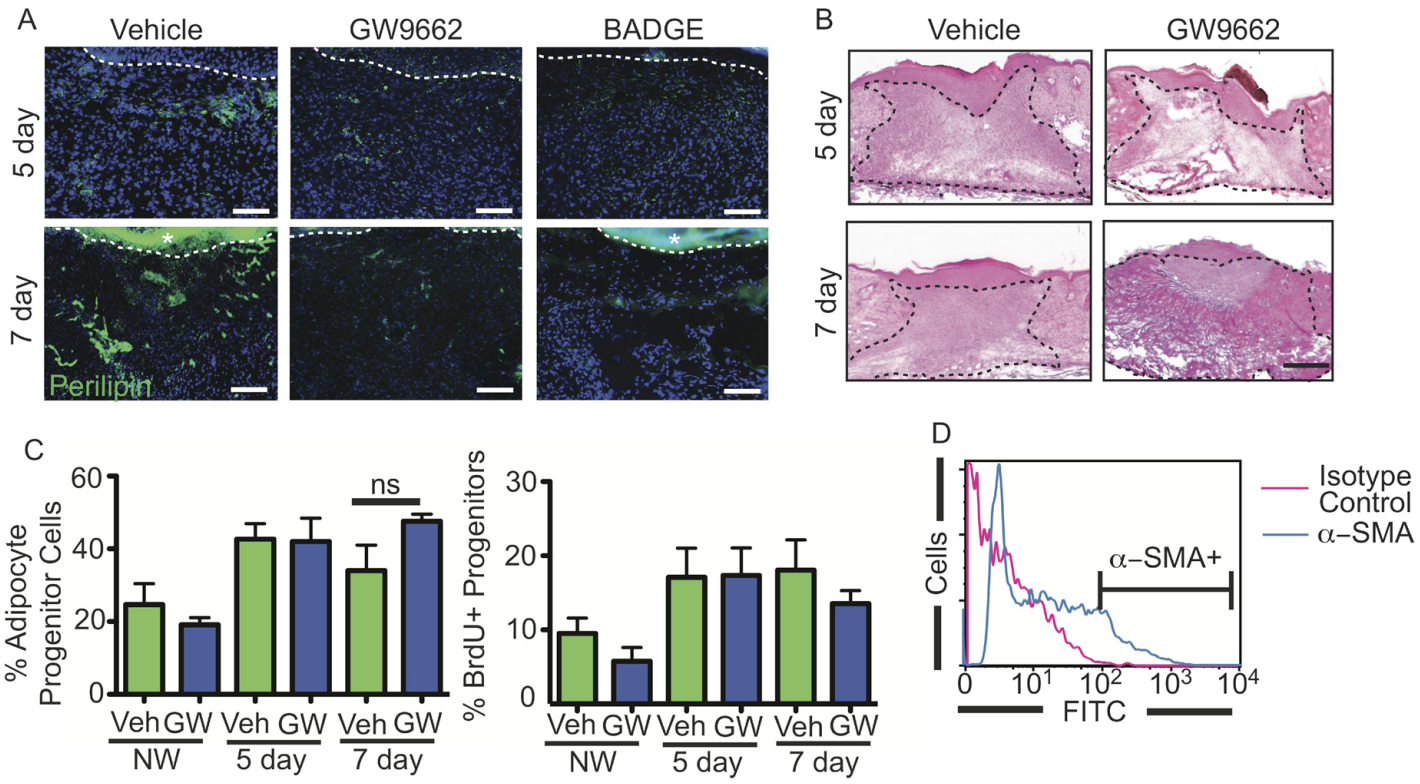

Fig. S3. Effect of GW9662 treatment on adipocyte lineage cells during wounding. (**A**) Lack of perilipin^{+}, mature adipocytes (green) in wounds of GW9662-injected and BADGE-injected mice 5 and 7 days after wounding compared with vehicle-injected mice as indicated. Dotted line indicates epidermal-dermal boundary. Asterisk indicates background staining. Scale bar: 100 μm. (**B**) H&E-stained skin sections of vehicle-injected and GW9662-injected wounds at 5 and 7 days after wounding showing abnormal dermal morphology. Dotted line outlines dermal wound bed. Scale bar: 200 μm. (**C**) The percentage of BrdU^{+} adipocyte progenitor cells is the same in GW9662-injected mice compared with the vehicle-injected control mice at 5 and 7 days after wounding. The percentage of adipocyte progenitor cells within the Lin^{-}, CD34^{+}, CD29^{+} cell population is the same in GW9662-treated mice compared with vehicle-injected controls. (**D**) FACS histogram plots of dermal cells isolated from skin wounds at day 5 stained with IgG2a-FITC (isotype control) or α-SMA-FITC antibodies. Line indicates + gate for α-SMA staining used in Fig. 4C.